

# van der Waals interaction in iron-chalcogenide superconductors

F. Ricci and G. Profeta

CNR-SPIN and Dipartimento di Scienze Fisiche e Chimiche, Università dell'Aquila, 67010 Coppito (L'Aquila), Italy

(Received 15 March 2013; revised manuscript received 18 April 2013; published 6 May 2013)

We demonstrate that the inclusion of van der Waals dispersive interaction sensibly improves the prediction of lattice constants by density functional theory in iron-chalcogenides (FeCh) superconductor compounds, namely FeSe and FeTe. We show how generalized gradient approximation (GGA) for the exchange correlation potential overestimates the out-of-plane lattice constants in both compounds when compared with experiments. In addition, GGA predicts a too weak bonding between the neutral FeCh layers, with a sensible underestimation of the bulk modulus. van der Waals corrected simulations completely solve both problems, reconciling theoretical results with experiments. These findings must be considered when dealing with theoretical predictions in FeCh compounds.

DOI: [10.1103/PhysRevB.87.184105](https://doi.org/10.1103/PhysRevB.87.184105)

PACS number(s): 74.70.Xa, 71.15.Nc, 61.50.Ah, 62.20.-x

## I. INTRODUCTION

The discovery of high-temperature superconductivity in iron pnictides (FePn)<sup>1,2</sup> raised a strong interest in searching for new superconducting materials which contain Fe and share common structural features with FePn superconductors. For example, superconductivity was found in the iron chalcogenide (FeCh) FeSe and its alloys when Se is partially substituted by Te.<sup>3</sup> The structure of FeCh is characterized by stack of neutral layers tetrahedrally coordinating Fe ions with chalcogens (Ch), similar in structure with respect to the FeAs layer in FePn's which, on the contrary, are negatively charged due to the presence of intercalates and oxides layers.<sup>4</sup> Despite lower critical temperature, the  $\text{Fe}_{1+y}\text{Se}_x\text{Te}_{1-x}$  family has a simpler crystal structure compared to those of FePn. For these reasons, the FeCh alloys can be considered as useful prototype systems to investigate the fundamental aspects of structural, electronic, magnetic, and superconducting properties in Fe-based superconductors.

Moreover, FeCh alloys show exceptional physical properties originating from the competing magnetic and superconducting orders. In particular, FeSe is superconductor with a transition temperature of  $T_c \sim 8$  K at ambient pressure,<sup>5</sup> which grows up to 37 K when the pressure reaches 9 GPa,<sup>6</sup> suggesting that the lattice plays a fundamental role in the superconducting transition. On the contrary, the parent FeTe crystal is not superconductor.<sup>7,8</sup> However, it was shown that 90-nm-thick films under tensile strain become superconductors with onset temperature at 13 K, confirming a sensible role of the lattice.<sup>9</sup>

First principles density functional theory (DFT) is considered a fundamental theoretical and computational tool to investigate the structural and electronic properties of the normal state of Fe-based superconductors.<sup>10,11</sup> Indeed, it was able to interpret the experimentally observed topology of the Fermi surfaces (FSs), the magnetic phases, and the structural distortion observed at low temperature.

In the early period of research, a strong interest was devoted to understanding the predicting power of DFT in both local density (LDA) and generalized gradient approximations (GGA),<sup>12</sup> showing the importance of magnetic correlation in the prediction of lattice constants. It was found that geometry optimizations performed considering a static Fe magnetic moment (although much higher than the measured one) generally mimic the magnetic fluctuations and correlations,<sup>13</sup> thus

predicting crystal lattice constants in acceptable agreement with experiments.<sup>14</sup>

However, a notable exception exists: *ab initio* DFT in both LDA and GGA approximation fails in predicting the lattice constants of FeCh crystal structures, in particular of the out-of-plane lattice constant.<sup>14</sup> Indeed, at present, most calculations have focused on the study of electronic properties considering the experimental measured lattice parameters with the only optimized quantity being the Ch height ( $h_{\text{Ch}}$ ) with respect to the Fe-atoms plane.<sup>3,10,15</sup> However, it must be emphasized that, due to the very simple layered structure, the equilibrium volume and  $h_{\text{Ch}}$  critically affect the electronic structure. Then, in order to predict the details of electronic properties of FeSe, FeTe, and their alloys from first principles in different physical conditions (alloys, pressure effect, surfaces, etc.), it results fundamental to properly solve the theoretical problems affecting the out-of-plane interaction between layers.

Although widely recognized,<sup>16</sup> the role of dispersive van der Waals (vdW) interactions between neutral FeSe and FeTe layers was not properly investigated.

It is well known that a general drawback of all common exchange and correlation functionals is that they do not properly describe long-range electronic correlations, as the vdW interaction.<sup>17-19</sup> In fact, computational investigations using DFT are not simply interpretable when studying systems in which vdW dispersion plays a crucial role due to nonlocal correlation effects.

Recently, a large effort was devoted to take into account vdW interactions and very interesting works were dedicated to point out the state-of-the-art in advanced materials.<sup>20</sup> For example, Hyldgaard, in an extensive review,<sup>20</sup> evaluated and established the limits and ranges of applicability of many different computational approaches developed to account for vdW on a large family of materials ranging from insulators, semiconductors, and metals.

In the present work, we show how first principles DFT successfully describe the crystal structure of FeSe and FeTe, with unprecedented agreement compared with experiments, once corrected to include the nonlocal vdW interaction, improving the calculation of out-of-plane lattice constant, interlayer binding energy, and bulk modulus. In addition, we show the effect of corrected lattice parameters in the electronic properties (band structure and Fermi surface) in both FeSe and FeTe.

## II. COMPUTATIONAL DETAILS

The calculations were performed using the Vienna Ab-Initio Simulation Package (VASP)<sup>21,22</sup> within the generalized gradient approximation (GGA).<sup>23</sup> The Perdew, Burke, and Ernzerhof (PBE)<sup>24</sup> functional was used to calculate the exchange-correlation potential. The GGA approximation correctly predicts the ground state magnetic phase for FeSe<sup>15</sup> and FeTe.<sup>25</sup> Winiarski *et al.*<sup>26</sup> showed that LDA estimates more precisely FeSe lattice constants than GGA; however, the calculations were performed in the PbO-type tetragonal nonmagnetic phase, neglecting fundamental structural distortions and magnetic effects. However, the relative success of the LDA in predicting the high temperature lattice parameters is merely due to an accidental cancellation of errors between the correlations and exchange energies.<sup>27</sup>

In this paper, we used projected augmented-wave (PAW) pseudopotentials<sup>28</sup> for all the atomic species involved and in order to achieve a satisfactory degree of convergence the  $3p^6 3d^6 4s^2$  states of Fe,  $4s^2 4p^4$  of Se, and  $5s^2 5p^4$  states of Te were treated as valence electrons with an energy cutoff up to 550 eV. Integrations over the Brillouin zone (BZ) were performed considering different uniform Monkhorst and Pack grids<sup>29</sup> depending on lattices:  $13 \times 13 \times 9$  and  $14 \times 7 \times 9$  for magnetic collinear stripe (AFM1) FeSe ( $a\sqrt{2} \times b\sqrt{2} \times c$  unit cell) and magnetic bicollinear double stripe (AFM2) FeTe ( $a \times 2b \times c$  crystal unit cell), respectively. For the tetragonal ( $a \times a \times c$ ) paramagnetic (PM) phase, which contains two Fe and two Ch atoms, we used  $20 \times 20 \times 15$  and  $15 \times 15 \times 9$   $k$ -grid for FeSe and FeTe, respectively.

The vdW interaction is considered using the DFT-D2 Grimme's semiempirical force-field correction<sup>30,31</sup> and the so-called vdW-optB86b functional as implemented in the VASP code.<sup>32</sup> The two functionals were chosen for their simplicity (DFT-D2) and high accuracy (vdW-optB86b).

Due to the high accuracy required in the calculations, we previously checked the pseudopotential quality with all-electron full potential linear augmented plane-wave method in the FLAIR implementation.<sup>33,34</sup> In Fig. 1 we show the

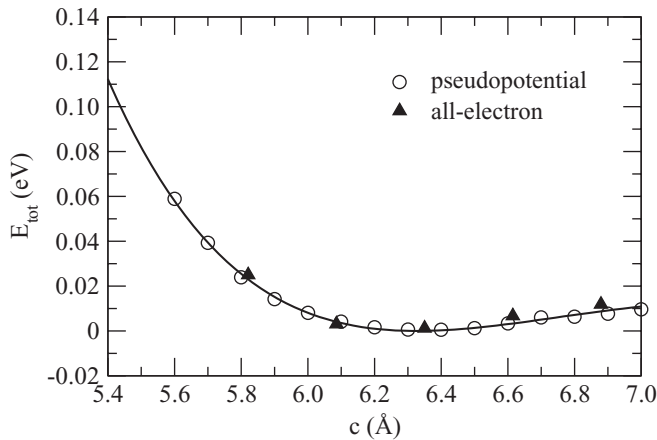


FIG. 1. Pseudopotential (open circles) and all-electron (full triangles) energy curves calculated for FeSe AFM1 phase as a function of  $c$  lattice constant. The in-plane  $a$  and  $b$  lattice constants are kept fixed at the experimental values.<sup>35</sup> The solid black line is a guide to the eyes.

TABLE I. Structural parameters and magnetic moments for FeSe and FeTe. Available experiments are also reported.

Expt.	$T$ (K)	$a$ (Å)	$b$ (Å)	$c$ (Å)	$h_{\text{Ch}}$ (Å)	$\alpha$ (deg)
FeSe <sup>35</sup>	7	3.7646	3.7540	5.479	1.4621	90.00
FeTe <sup>36</sup>	2	3.8312	3.7830	6.264	1.7540	89.17
GGA		$a$ (Å)	$b$ (Å)	$c$ (Å)	$h_{\text{Ch}}$ (Å)	$\alpha$ (deg)
FeSe	PM	3.68	3.68	6.26	1.39	90.00
FeTe		3.81	3.81	6.52	1.59	90.00
FeSe	AFM	3.75	3.71	6.32	1.45	90.00
FeTe		3.87	3.63	6.90	1.78	86.60
DFT-D2		$a$ (Å)	$b$ (Å)	$c$ (Å)	$h_{\text{Ch}}$ (Å)	$\alpha$ (deg)
FeSe	PM	3.64	3.64	5.42	1.40	90.00
FeTe		3.77	3.77	6.03	1.59	90.00
FeSe	AFM	3.67	3.61	5.53	1.46	90.00
FeTe		3.81	3.61	6.42	1.77	88.53

$c$ -axis relaxation, fixing the in-plane lattice parameter to experimental values (see below and Table I for all details and references) on AFM1 FeSe for VASP and FLAIR simulations. The pseudopotential energy curve nicely agrees with the all-electron one in a wide range of  $c$  lattice constant, giving equilibrium  $c$  of 6.30 and 6.25, respectively. This is a fundamental consistence check due to the already discussed issues related to the comparison between all-electron within the well converged pseudopotentials.<sup>12</sup>

## III. RESULTS AND DISCUSSION

Having tested the accuracy of pseudopotentials, we calculated the energy-volume phase diagrams for FeSe and FeTe in both PM and AFM configurations with and without the vdW correction. The results (with available experimental measurements) are presented in Table I and Figs. 2 and 3.

Since the PM calculations neglect magnetic interactions, fundamental to reproducing experiments, we will mainly focus our attention on AFM phases.

In both FeSe and FeTe the GGA curves show a very weak interaction between the layers, predicting a too large lattice  $c$  constant when compared with experiments. As we can see, for FeSe (FeTe) the GGA gives a  $\sim 15\%$  ( $10\%$ ) deviation from experiments for the out-of-plane  $c$  lattice constant, while the in-plane  $a$  and  $b$  parameters are in good agreement with a deviation lower than 1% (4%).

On the contrary, the interlayer bonding energy, corrected with the semiempirical DFT-D2 vdW dispersion potential, shifts the minimum of the total energy indicating an increased interaction between FeCh layers, shrinking all the lattice parameters with respect to GGA. In FeSe and FeTe  $a$  and  $b$  remain consistent with experimental values in a range of  $\sim 0\%$ – $5\%$ , depending on material, while along the  $c$  axis, there is a sensible improvement: the theoretical value is corrected within 1%–3% with respect to experiments. Moreover, it is very interesting to note that, for the FeTe AFM phase, the DFT-D2 improve also the monoclinic  $\alpha$  angle.

We have fitted the curves with a Birch-Murnaghan equation of state,<sup>37</sup> and compare the equilibrium volumes and the bulk moduli (shown in Table II) with available experiments.

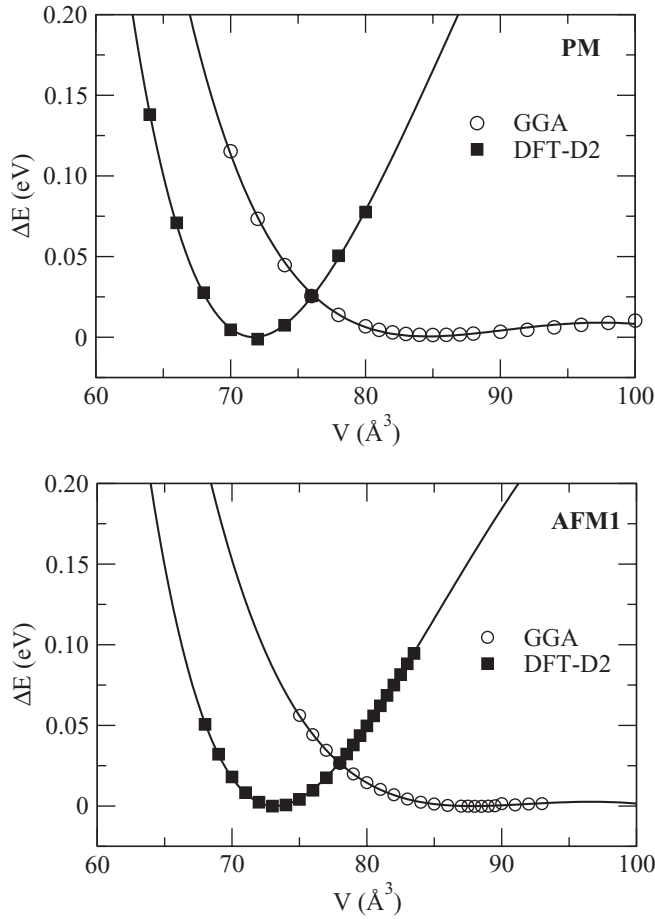


FIG. 2. FeSe energy-volume curves for GGA (open circles) and vdW DFT-D2 (full squares) in the PM (upper panel) and AFM1 (lower panel) phases. Volume and energies refer to the conventional unit cell. Solid lines are the fitted Birch-Murnaghan equation of state.<sup>37</sup>

The most evident result is the striking disagreement between GGA and experimental bulk moduli for both FeSe and FeTe. In fact, as evident from Figs. 2 and 3, the out-of-plane interaction is too weak resulting in a very low  $B_0$ . This behavior is dependent on the magnetic phase considered. Interestingly, we observe that the vdW correction completely changes the physics and chemistry of the out-of-plane interaction thus resulting in a much better agreement with experiments. We note that, even in this case, both PM and AFM phases are corrected in the same way. The overall satisfactory agreement indicates that the vdW interlayer interaction is fundamental to correctly reproducing the properties of FeCh compounds.

As evident from our results, and as already well discussed in review articles (see, for example, Refs. 17, 18, and 20), the main effect of the vdW interaction is the  $c$  lattice constant reduction and the consequent increase of  $B_0$ , an effect common to other layered materials.

In recent reviews,<sup>20</sup> it was shown as different approaches to include the vdW interaction can lead to different calculated lattice constants. The DFT-D2 is a semiempirical method, very efficient, but relies on the optimization of four semiempirical parameters,<sup>30</sup> previously fitted on different classes of materials.<sup>31</sup> In order to further investigate vdW functionals, we used the so-called vdW-optB86b,<sup>32,40</sup> which

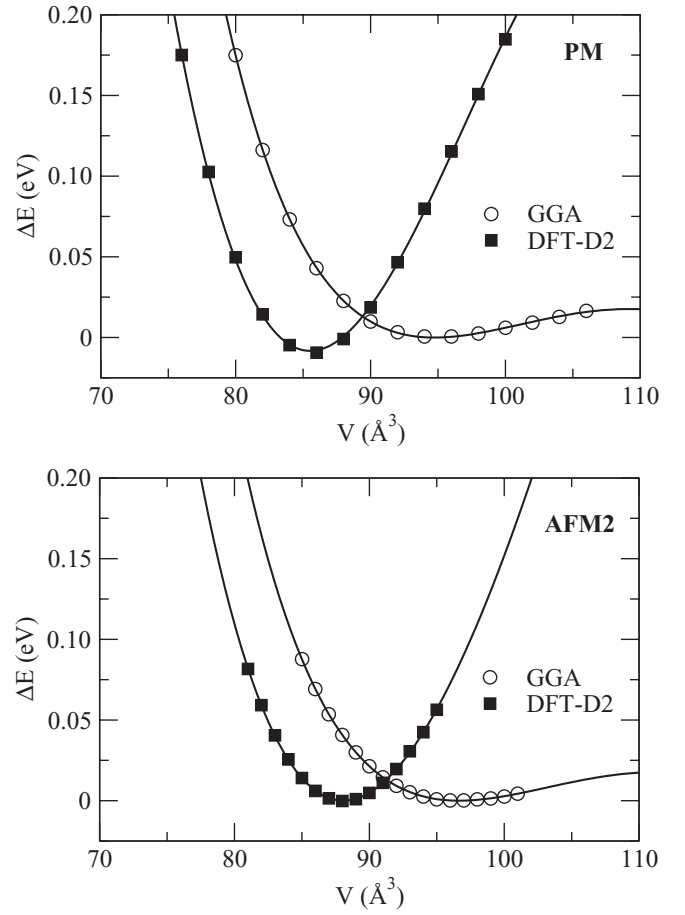


FIG. 3. FeTe energy-volume curves for GGA (open circles) and vdW DFT-D2 (full squares) in the PM (upper panel) and AFM2 (lower panel) phases. Volume and energies refer to the conventional unit cell. Solid lines are the fitted Birch-Murnaghan equation of state.<sup>37</sup>

includes the nonlocal vdW interaction in the exchange and correlation energy functionals. This method was demonstrated to have a wide range of applicability and excellent agreement

TABLE II. Equilibrium volumes and bulk moduli of the conventional cell calculated for paramagnetic (PM) and antiferromagnetic (AFM: AFM1 and AFM2 for FeSe and FeTe, respectively) phases with and without vdW correction.

Expt.	$T$ (K)	$V_{eq}$ ( $\text{\AA}^3$ )	$B_0$ (GPa)
FeSe <sup>38</sup>	50	77.56	33
FeTe <sup>39</sup>	300	91.98	36
		$V_{eq}$ ( $\text{\AA}^3$ )	$B_0$ (GPa)
GGA			
FeSe	PM	84.95	5.28
FeTe		94.73	9.81
FeSe	AFM	87.82	3.37
FeTe		96.65	9.71
		$V_{eq}$ ( $\text{\AA}^3$ )	$B_0$ (GPa)
DFT-D2			
FeSe	PM	71.73	37.57
FeTe		85.53	36.46
FeSe	AFM	73.18	34.67
FeTe		88.08	38.99

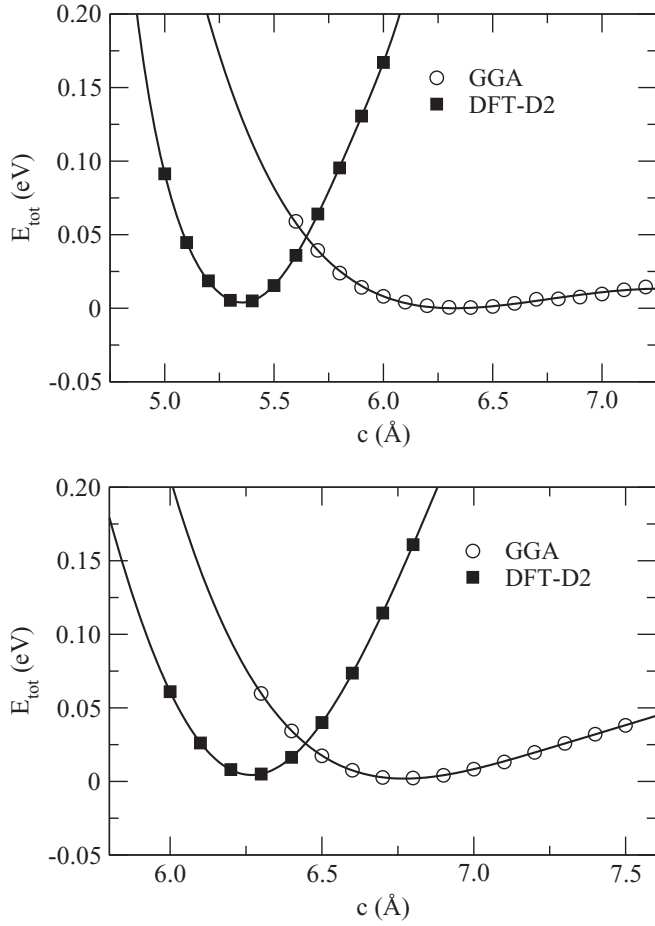


FIG. 4. AFM1 FeSe (upper panel) and AFM2 FeTe (lower panel)  $c$ -relaxed total energy GGA (open circles) and DFT-D2 (full squares) curves. The solid lines are shown as guides for the eyes.

with experimental results on different solids in terms of lattice constants, bulk moduli, and atomization energies. We performed lattice parameters and internal coordinates optimization varying independently  $a$  and  $c$  and compared the results with DFT-D2 method. The results show the complete consistency of the two approaches.

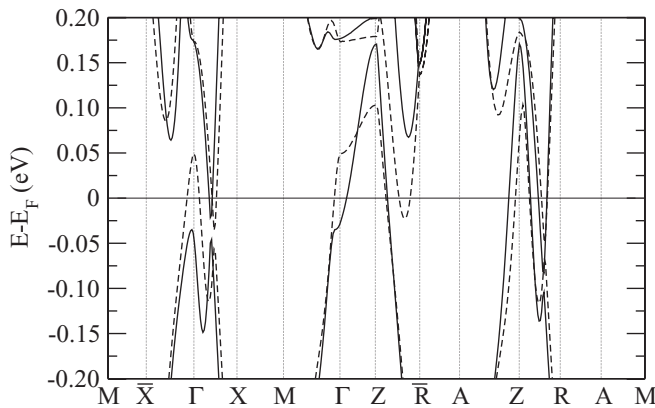


FIG. 5. FeSe band structure calculated using the GGA (dashed lines) and DFT-D2 (solid lines) lattice constants.

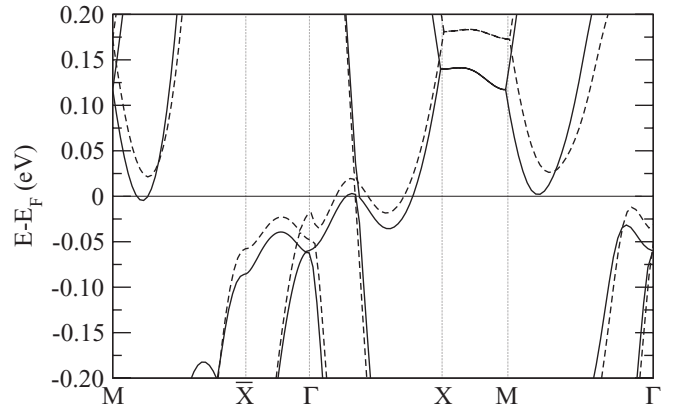


FIG. 6. FeTe band structure calculated using the GGA (dashed lines) and DFT-D2 (solid lines) lattice constants.

The use of the corrected  $c$  lattice constant has a strong effect on band structure and FS near the Fermi energy. In order to understand this effect on electronic properties, we calculated the band structure and FSs for AFM FeSe and FeTe considering both GGA and DFT-D2 relaxed  $c$  lattice constants. To disentangle the (small) differences in the in-plane lattice parameters (see Table I), we calculated the equilibrium  $c$  constant fixing both  $a$  and  $b$  ones to experimental values. This is a well justified procedure to predict interlayer distance widely used in literature in the case of layered crystals in which the strongest vdW correction comes from the out-of-plane interaction.<sup>17,18</sup>

Figure 4 shows the theoretical results obtained in this way for AFM FeSe and FeTe phases which are compatible with experiments in a range around 2% and 0.1% for the FeSe and FeTe, respectively.

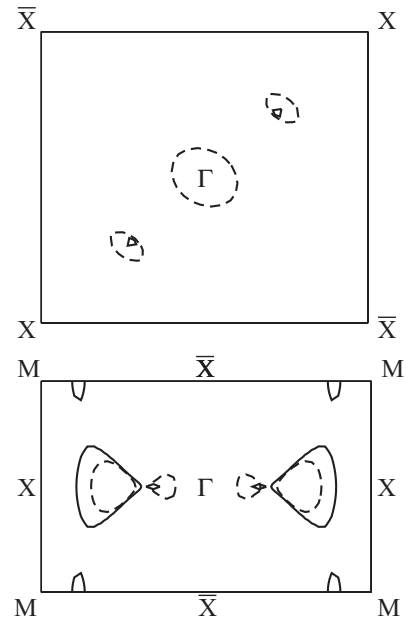


FIG. 7. FeSe and FeTe Fermi surfaces (upper and lower panel, respectively) calculated using GGA (dashed line) and DFT-D2 (solid line) lattice constants.



In Figs. 5 and 6 we show the band structures calculated for the FeSe and FeTe using the above lattice constants, and in Fig. 7 the relative FSs. Considering the GGA  $c$  parameter, we observe in FeSe a hole pocket at the  $\Gamma$  point and two very small electron ones along the  $\Gamma X$  direction. In particular, these two pockets are related to the presence of a Dirac-like point just below the Fermi energy. A nearly Dirac point is also present on the  $c^*/2$  plane, along the ZR line. The electronic states change sensibly using the predicted  $c$  lattice constant with vdW correction: the hole pocket at the  $\Gamma$  point is now completely filled, while the Dirac point along the  $\Gamma X$  line shifts nearer  $E_F$ , closing all FSs in the  $\Gamma XM$  plane.

In FeTe we observe that hole and electron pockets along the  $\Gamma X$  for the GGA  $c$  lattice constant transforms in the electron pocket completely filling the hole one, once vdW parameters are considered.

In conclusion, we studied the effect of the vdW correction on the calculation of lattice constants and bulk modulus of

FeCh superconductors. We showed that the vdW correction is fundamental in order to predict lattice structure and bulk moduli in agreement with the experiments, having a large effect on the out-of-plane bonding between the Ch-Fe-Ch layers.

These results are important in view of computational experiments within first-principles DFT methods on Fe-based superconductors and can also be extended to predict the effect of substitutions, intercalations, high pressure, strain, and surface effects on the structural, electronic, and magnetic properties of these compounds.

## ACKNOWLEDGMENTS

This work was supported by FP7 European project SUPER-IRON (Grant Agreement No. 283204). The work was supported by a CINECA-HPC ISCRA grant and by an HPC grant at CASPUR.

- <sup>1</sup>Y. Kamihara, T. Watanabe, M. Hirano, and H. Hosono, *J. Am. Chem. Soc.* **130**, 3296 (2008).
- <sup>2</sup>Z. A. Ren, W. Lu, J. Yang, W. Yi, X.-L. Shen, Z.-C. Li, G.-C. Che, X.-L. Dong, L.-L. Sun, F. Zhou, and Z.-X. Zhao, *Chin. Phys. Lett.* **25**, 2215 (2008).
- <sup>3</sup>A. Subedi, L. Zhang, D. J. Singh, and M. H. Du, *Phys. Rev. B* **78**, 134514 (2008).
- <sup>4</sup>G. R. Stewart, *Rev. Mod. Phys.* **83**, 1589 (2011).
- <sup>5</sup>F. C. Hsu, J. Y. Luo, K. W. Yeh, T.-K. Chen, T. W. Huang, P. M. Wu, Y. C. Lee, Y. L. Huang, Y. Yi Chu, D. C. Yan, and M. K. Wu, *Proc. Natl. Acad. Sci. USA* **105**, 14262 (2008).
- <sup>6</sup>S. Medvedev, T. M. McQueen, I. A. Troyan, T. Palasyuk, M. I. Eremets, R. J. Cava, S. Naghavi, F. Casper, V. Ksenofontov, G. Wortmann, and C. Felser, *Nat. Mater.* **8**, 630 (2009).
- <sup>7</sup>Y. Mizuguchi, F. Tomioka, S. Tsuda, T. Yamaguchia, and Y. Takano, *Physica C: Supercond.* **469**, 1027 (2009).
- <sup>8</sup>H. Takahashi, H. Takahashi, T. Tomita, H. Okada, Y. Mizuguchi, Y. Takano, S. Matsui, M. Hirano, and H. Hosono, *Jpn. J. Appl. Phys.* **50**, 05FD01 (2011).
- <sup>9</sup>Y. Han, W. Y. Li, L. X. Cao, X. Y. Wang, B. Xu, B. R. Zhao, Y. Q. Guo, and J. L. Yang, *Phys. Rev. Lett.* **104**, 017003 (2010).
- <sup>10</sup>P. P. Singh, *J. Phys.: Condens. Matter* **22**, 135501 (2010).
- <sup>11</sup>M. D. Johannes, I. I. Mazin, and D. S. Parker, *Phys. Rev. B* **82**, 024527 (2010).
- <sup>12</sup>I. I. Mazin, M. D. Johannes, L. Boeri, K. Koepernik, and D. J. Singh, *Phys. Rev. B* **78**, 085104 (2008).
- <sup>13</sup>M. Liu, L. W. Harriger, H. Luo, M. Wang, R. A. Ewings, T. Guidi, H. Park, K. Haule, G. Kotliar, S. M. Hayden, and P. Dai, *Nature Phys.* **8**, 376 (2012).
- <sup>14</sup>F. Caglieris, F. Ricci, G. Lamura, A. Martinelli, A. Palenzona, I. Pallecchi, A. Sala, G. Profeta, and M. Putti, *Sci. Technol. Adv. Mater.* **13**, 054402 (2012).
- <sup>15</sup>H. Shi, Z. Huang, J. S. Tse, and H. Q. Lin, *J. Appl. Phys.* **110**, 043917 (2011).
- <sup>16</sup>Y. Mizuguchi and Y. Takano, *J. Phys. Soc. Jpn.* **79**, 102001 (2010).
- <sup>17</sup>T. Björkman, A. Gulans, A. V. Krashennnikov, and R. M. Nieminen, *J. Phys.: Condens. Matter* **42**, 424218 (2012).
- <sup>18</sup>T. Björkman, *Phys. Rev. B* **86**, 165109 (2012).
- <sup>19</sup>T. Björkman, A. Gulans, A. V. Krashennnikov, and R. M. Nieminen, *Phys. Rev. Lett.* **108**, 235502 (2012).
- <sup>20</sup>Special issue on van der Waals interactions in advanced materials [*J. Phys. Condens. Matter* **42** (2012)].
- <sup>21</sup>G. Kresse and J. Furthmüller, *Phys. Rev. B* **54**, 11169 (1996).
- <sup>22</sup>G. Kresse and J. Furthmüller, *Comput. Mater. Sci.* **6**, 15 (1996).
- <sup>23</sup>G. Kresse and D. Joubert, *Phys. Rev. B* **59**, 1758 (1999).
- <sup>24</sup>J. P. Perdew, K. Burke, and M. Ernzerhof, *Phys. Rev. Lett.* **77**, 3865 (1996).
- <sup>25</sup>S. Li, C. de la Cruz, Q. Huang, Y. Chen, J. W. Lynn, J. Hu, Y. L. Huang, F. C. Hsu, K. W. Yeh, M. K. Wu, and P. Dai, *Phys. Rev. B* **79**, 054503 (2009).
- <sup>26</sup>M. J. Winiarski, M. Samsel-Czekala, and A. Ciechan, *Europhys. Lett.* **100**, 47005 (2012).
- <sup>27</sup>A. Marini, P. García-González, and A. Rubio, *Phys. Rev. Lett.* **96**, 136404 (2006).
- <sup>28</sup>P. E. Blöchl, *Phys. Rev. B* **50**, 17953 (1994).
- <sup>29</sup>H. J. Monkhorst and J. D. Pack, *Phys. Rev. B* **13**, 5188 (1976).
- <sup>30</sup>S. Grimme, *J. Comput. Chem.* **27**, 1787 (2006).
- <sup>31</sup>In the DFT-D2 method of Grimme, the van der Waals interaction is described adding a semiempirical dispersion potential to the Kohn-Sham energies:

$$E_{\text{disp}} = -\frac{s_6}{2} \sum_{i=1}^{N_{\text{at}}} \sum_{j=1}^{N_{\text{at}}} \sum_{\mathbf{L}} \frac{C_6^{ij}}{|\mathbf{r}_i^{(i,0)} - \mathbf{r}_j^{(i,\mathbf{L})}|} f\left(\left|\mathbf{r}_i^{(i,0)} - \mathbf{r}_j^{(i,\mathbf{L})}\right|\right), \quad (1)$$

where  $N_{\text{at}}$  is the overall number of atoms,  $\mathbf{L}$  represents all possible translations of the unit cell (within  $i \neq j$  for  $L = 0$ ),  $s_6$  a global scaling factor,  $C_6^{ij}$  the dispersion coefficient for the  $ij$  pair,  $\mathbf{r}_i^{i,\mathbf{L}}$  the position vector of atom  $i$  in the  $L$ th unit cell, and  $f$  a damping function containing a damping  $d$  factor and the vdW radius  $R_0$ . The parameters we used were as follows: for Fe we used  $C_6 = 10.800 \text{ J nm}^6 \text{ mol}^{-1}$  and  $R_0 = 1.562 \text{ Å}$ , for Se  $C_6 = 12.640 \text{ J nm}^6 \text{ mol}^{-1}$  and  $R_0 = 1.771 \text{ Å}$ , and for Te  $C_6 = 31.740 \text{ J nm}^6 \text{ mol}^{-1}$  and  $R_0 = 1.892 \text{ Å}$ . For  $d$  and  $s_6$  we used  $20.00 \text{ Å}$  and  $0.75$ , respectively.

- <sup>32</sup>J. Klimeš, D. R. Bowler, and A. Michaelides, *Phys. Rev. B* **83**, 195131 (2011).
- <sup>33</sup>H. J. F. Jansen and A. J. Freeman, *Phys. Rev. B* **30**, 561 (1984).
- <sup>34</sup>E. Wimmer, H. Krakauer, M. Weinert, and A. J. Freeman, *Phys. Rev. B* **24**, 864 (1981).
- <sup>35</sup>D. Louca, K. Horigane, A. Llobet, R. Arita, S. Ji, N. Katayama, S. Konbu, K. Nakamura, T.-Y. Koo, P. Tong, and K. Yamada, *Phys. Rev. B* **81**, 134524 (2010).
- <sup>36</sup>A. Martinelli, A. Palenzona, M. Tropeano, C. Ferdeghini, M. Putti, M. R. Cimberle, T. D. Nguyen, M. Affronte, and C. Ritter, *Phys. Rev. B* **81**, 094115 (2010).
- <sup>37</sup>F. D. Murnaghan, *Proc. Natl. Acad. Sci. USA* **30**, 244 (1944).
- <sup>38</sup>J. N. Millican, D. Phelan, E. L. Thomas, J. B. Leão, and E. Carpenter, *Solid State Commun.* **149**, 707 (2009).
- <sup>39</sup>J. E. Jørgensen, J. Staun Olsen, and L. Gerward, *High Press. Res.* **31**, 603 (2011).
- <sup>40</sup>J. Klimeš and A. Michaelides, *J. Chem. Phys.* **137**, 120901 (2012).